Secreted Fungal Effector Lipase Releases Free Fatty Acids to Inhibit Innate Immunity-Related Callose Formation during Wheat Head Infection[W][OPEN]

Antje Blümke[1], Christian Falter[1], Cornelia Herrfurth, Björn Sode, Rainer Bode, Wilhelm Schäfer, Ivo Feussner, and Christian A. Voigt*

Molecular Phytopathology and Genetics, Biocenter Klein Flottbek, University of Hamburg, 22609 Hamburg, Germany (A.B., C.F., B.S., W.S., C.A.V.); and Department of Plant Biochemistry, Albrecht von Haller Institute for Plant Sciences, Georg August University, 37077 Goettingen, Germany (C.H., R.B., I.F.)

The deposition of the (1,3)-β-glucan cell wall polymer callose at sites of attempted penetration is a common plant defense response to intruding pathogens and part of the plant's innate immunity. Infection of the *Fusarium graminearum* disruption mutant Δ*fgl1*, which lacks the effector lipase FGL1, is restricted to inoculated wheat (*Triticum aestivum*) spikelets, whereas the wild-type strain colonized the whole wheat spike. Our studies here were aimed at analyzing the role of FGL1 in establishing full *F. graminearum* virulence. Confocal laser-scanning microscopy revealed that the Δ*fgl1* mutant strongly induced the deposition of spot-like callose patches in vascular bundles of directly inoculated spikelets, while these callose deposits were not observed in infections by the wild type. Elevated concentrations of the polyunsaturated free fatty acids (FFAs) linoleic and α-linolenic acid, which we detected in *F. graminearum* wild type-infected wheat spike tissue compared with Δ*fgl1*-infected tissue, provided clear evidence for a suggested function of FGL1 in suppressing callose biosynthesis. These FFAs not only inhibited plant callose biosynthesis in vitro and in planta but also partially restored virulence to the Δ*fgl1* mutant when applied during infection of wheat spikelets. Additional FFA analysis confirmed that the purified effector lipase FGL1 was sufficient to release linoleic and α-linolenic acids from wheat spike tissue. We concluded that these two FFAs have a major function in the suppression of the innate immunity-related callose biosynthesis and, hence, the progress of *F. graminearum* wheat infection.

The molecular and physiological regulation of the biosynthesis of callose, which is a (1,3)-β-glucan polymer with some (1,6)-branches (Aspinall and Kessler, 1957), and its importance for plant development as well as plant defense are still under examination. Regarding the involvement of callose in plant defense responses, particular attention has been focused on the formation of cell wall thickenings in plants, so-called papillae, at sites of microbial attack. They were already described 150 years ago (deBary, 1863) and reported to commonly contain callose (Mangin, 1895). Since then, examinations have identified callose as the most abundant chemical constituent in papillae, which may also include proteins (e.g. peroxidases and antimicrobial thionins), phenolics, and other constituents (Aist and Williams, 1971; Sherwood and Vance, 1976; Mims et al., 2000). Papillae have been regarded as an early defense reaction that may not completely stop the pathogen; rather, they have been considered to act as a physical barrier to slow pathogen invasion (Stone and Clarke, 1992; Voigt and Somerville, 2009) and to contribute to the plant's innate immunity (Jones and Dangl, 2006; Schwessinger and Ronald, 2012). The host plant can gain time to initiate defense reactions that require gene activation and expression, such as the hypersensitive reactions, phytoalexin production, and pathogenesis-related protein synthesis (Lamb and Dixon, 1997; Brown et al., 1998). However, our recent study revealed that callose can also act as a barrier that completely prevents fungal penetration. The overexpression of *POWDERY MILDEW RESISTANT4* (*PMR4*), a gene encoding a stress-induced callose synthase, resulted in early elevated callose deposition at sites of attempted powdery mildew penetration in Arabidopsis (*Arabidopsis thaliana*; Ellinger et al., 2013). Interestingly, the *pmr4* deletion mutant also showed an increased resistance to powdery mildew that, however, was induced at later stages of powdery mildew infection because an initial fungal penetration still occurred. In fact, the absence of the functional callose synthase PMR4 in the *pmr4* mutant resulted in papillae that were free from callose but also induced a hyperactivation of the salicylic acid defense pathway, which was shown to be the basis of resistance in double mutant and microarray analyses (Jacobs et al., 2003; Nishimura et al., 2003). The callose synthase gene *PMR4* from Arabidopsis belongs to the *GLUCAN SYNTHASE-LIKE* (*GSL*) family, genes that have been identified in higher plants including wheat (*Triticum aestivum*; Cui et al., 2001;

[1] These authors contributed equally to the article.

* Address correspondence to christian.voigt@uni-hamburg.de.

The author responsible for distribution of materials integral to the findings presented in this article in accordance with the policy described in the Instructions for Authors (www.plantphysiol.org) is: Christian A. Voigt (christian.voigt@uni-hamburg.de).

[W] The online version of this article contains Web-only data.

[OPEN] Articles can be viewed online without a subscription.

www.plantphysiol.org/cgi/doi/10.1104/pp.114.236737

Doblin et al., 2001; Hong et al., 2001; Østergaard et al., 2002; Voigt et al., 2006). The predicted function of these genes as callose synthases is generally supported by homology with the yeast *FK506 SENSITIVITY* (*FKS*) genes, which are believed to be subunits of (1,3)-β-glucan synthase complexes (Douglas et al., 1994; Dijkgraaf et al., 2002). Additionally, the predicted proteins encoded by the *GSL* genes correlate with the approximately 200-kD catalytic subunit of putative callose synthases. Li et al. (2003) showed that the amino acid sequence predicted from a *GSL* gene in barley (*Hordeum vulgare*; *HvGSL1*) correlates with the amino acid sequence of an active (1,3)-β-glucan synthase fraction.

In this study, we aimed to examine the involvement of callose synthesis and callose deposition in plant defense against intruding fungal pathogens in the pathosystem wheat-*Fusarium graminearum*. We focused on the ability of wheat to inhibit a further spread of fungal pathogens after an initial, successful infection. This resistance to fungal spread within the host has been referred to as type II resistance and is part of a widely accepted two-component system of resistance, which includes type I resistance operating against initial infection (Schroeder and Christensen, 1963). For our analyses, we used the direct interaction between wheat as host and *F. graminearum* as a pathogen. On the one hand, *Fusarium* head blight (FHB) of wheat, caused by *F. graminearum*, is one of the most destructive crop diseases worldwide (McMullen et al., 1997; del Blanco et al., 2003; Madgwick et al., 2011) and classifies this fungus as a top 10 plant pathogen based on its importance in science and agriculture (Dean et al., 2012). On the other hand, only a limited number of wheat cultivars were identified that revealed FHB resistance. However, these cultivars did not qualify for commercial cultivation or breeding approaches due to inappropriate agronomic traits (Buerstmayr et al., 2009). Further elucidation of the mechanisms of spreading resistance could support the generation of FHB-resistant wheat cultivars.

In this regard, we demonstrated that the secreted lipase FGL1 of *F. graminearum* is a virulence factor required for wheat infection (Voigt et al., 2005). A strong resistance to fungal spread was observed in a susceptible wheat cultivar after infection with the lipase-deficient *F. graminearum* strain Δ*fgl1*. Light microscopy indicated barrier formation in the transition zone of rachilla and rachis of directly inoculated spikelets. In contrast, neither spreading resistance nor barrier formation was observed during *F. graminearum* wild type infection. An active role of lipases in establishing full virulence was also recently proposed for the plant pathogen *Fusarium oxysporum* f. sp. *lycopersici*, where reduced lipolytic activity due to the deletion of lipase regulatory genes resulted in reduced colonization of tomato (*Solanum lycopersicum*) plants (Bravo-Ruiz et al., 2013). Because the expression of the lipase-encoding gene *LIP1* was induced in the biotrophic fungus *Blumeria graminis* during early stages of infection (Feng et al., 2009) and disruption of the putative secreted lipase gene *lipA* resulted in reduced virulence of the bacterial plant pathogen *Xanthomonas campestris* (Tamir-Ariel et al., 2012), a general importance of extracellular lipolytic activity during plant colonization is indicated.

We evaluated a possible role of callose in plant defense by infecting wheat spikes with the virulent fungal pathogen *F. graminearum* wild type, the virulence-deficient *F. graminearum* deletion mutant Δ*fgl1*, and the barley leaf pathogen *Pyrenophora teres*, the latter intended to induce strong plant defense responses as known from incompatible, nonhost interactions. The formation of callose plugs within the vascular bundles of inoculated spikelets and the callose synthase activity of infected spikelet tissue correlated directly with increased plant resistance. Subsequent analyses of free fatty acid (FFA) concentrations revealed that those polyunsaturated FFAs were enriched during wheat infection with the *F. graminearum* wild-type strain that could inhibit callose synthase activity in vitro as well as in planta and partially restored the virulence of the lipase-deficient *F. graminearum* strain Δ*fgl1*. On the basis of these results, we propose a model for FHB where defense-related callose synthase is inhibited by specific FFAs whose accumulation is caused by the fungus during fungal infection; this inhibition is required for full infection of the wheat head.

RESULTS

Callose Deposition in Wheat Spikes during Infection

Wheat spikes were inoculated with *F. graminearum* wild type, the lipase-deficient *F. graminearum* strain Δ*fgl1-2*, and the barley leaf pathogen *P. teres*. Water-inoculated spikelets served as controls. We stained sections of the transition zone of rachilla and rachis of directly inoculated spikelets with aniline blue to visualize callose depositions and with Alexa Fluor 488-conjugated wheat germ agglutinin to localize fungal hyphae in colonized tissue (Fig. 1A; Supplemental Fig. S1). Whereas we did not observe fungal hyphae in the transition of rachilla and rachis (Fig. 1B) at 1 d post inoculation (dpi), single hyphae of *F. graminearum* wild type and Δ*fgl1-2* entered this region at 3 dpi. At 7 dpi, the strongest colonization of the spikelet's transition zone occurred during *F. graminearum* wild type infection, but also Δ*fgl1-2* revealed a relatively strong colonization compared with the nonadapted fungal pathogen *P. teres* (Fig. 1A). The colonization of the transition zone of rachilla and rachis was accompanied by localized deposition of callose plugs within the vascular bundles of Δ*fgl1-2*- and *P. teres*-infected spikelets (Fig. 1A), which started at 3 dpi and peaked at 7 dpi (Fig. 1C). This localized callose deposition in the vascular tissue was absent in spikelets infected with *F. graminearum* wild type (Fig. 1, A and C; Supplemental Fig. S1). Higher magnification of aniline blue-stained vascular bundles revealed that the localized, pathogen-induced callose deposition in Δ*fgl1-2*- and *P. teres*-infected spikelets occurred in sieve elements of the phloem. Here, callose plugs could reach a size to block the respective sieve element. Interestingly, the pathogen-induced callose deposition was independent of the regularly observed

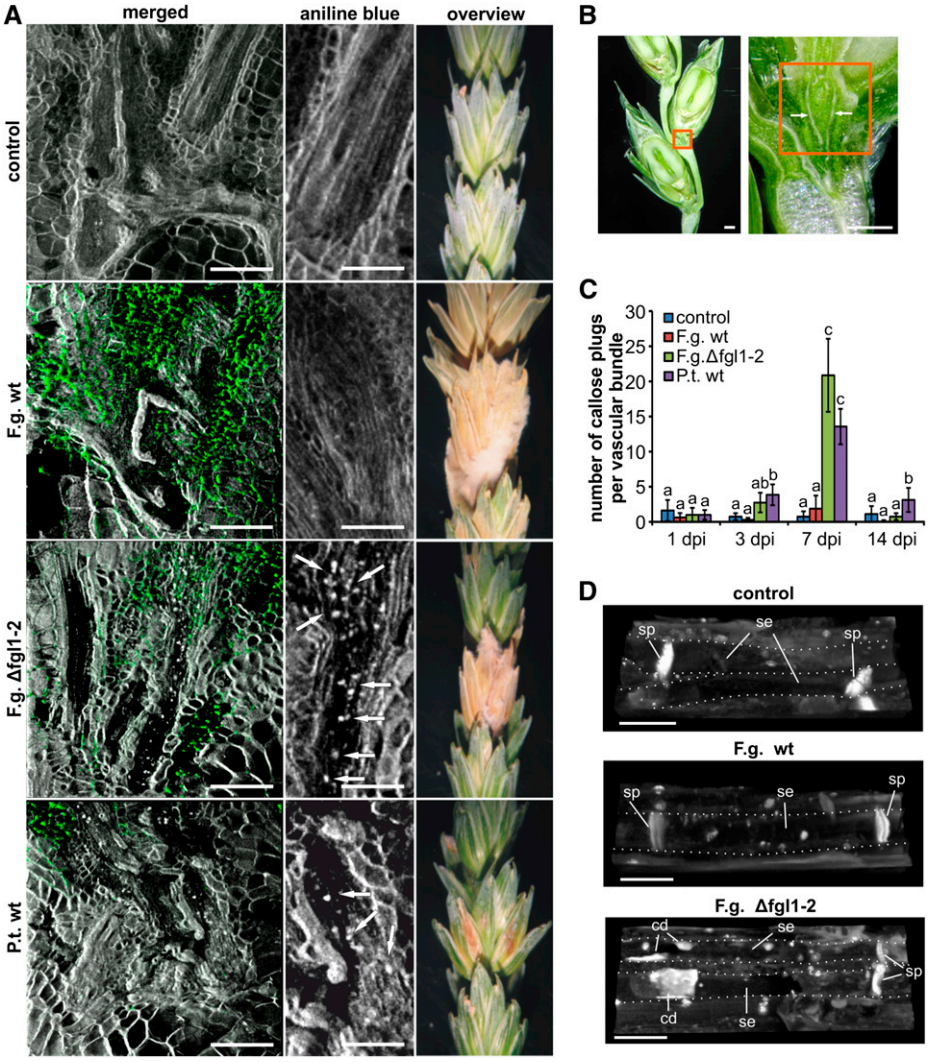

Figure 1. Callose deposition in wheat spikes after fungal infection. A, Sections of directly inoculated wheat spikelet comprising the transition zone of rachilla and rachis including vascular bundles, as indicated in B, at 7 dpi with *F. graminearum* wild type (F.g. wt), lipase-deficient strain Δ*fgl1-2* (F.g. Δfgl1-2), and *P. teres* wild type (P.t. wt). Untreated spikelets served as controls. Micrographs were taken by confocal laser-scanning microscopy. Green color was assigned to fungal hyphae stained with Alexa Fluor 488-conjugated wheat germ agglutinin, and grayscale was assigned to aniline blue-stained callose. Green and grayscale channels were merged for an overview of fungal colonization of spikelet tissue, and grayscale only (aniline blue) was used to highlight callose plugs (white arrows) in the phloem of vascular bundles of the transition zone. Micrographs are representative for infection at 7 dpi. Bars = 200 μm (left column) and 100 μm (middle column). The right column provides a macroscopic overview of the disease severity of directly inoculated spikelets at 14 dpi. B, Longitudinal section of wheat spikelets and rachis to highlight the transition zone of rachilla and rachis including vascular bundles (white arrows). The orange frame indicates the area of microscopic analysis in A. Bars = 1 mm. C, Number of callose plugs located in the phloem of vascular bundles of the transition zone of rachilla and rachis tissue from directly inoculated spikelets as analyzed in A at 1, 3, 7, and 14 dpi with *F. graminearum* wild type, lipase-deficient strain Δ*fgl1-2*, and *P. teres* wild type. Untreated spikelets served as controls. Values represent means of eight biologically independent inoculation experiments for each fungal strain. The letters a, b, and c indicate $P < 0.05$ by Tukey's test. Error bars represent SE, and $n = 8$. D, High-resolution microscopy of callose deposition (fluorescence by aniline blue staining) in sieve elements (indicated by dotted lines) of the phloem in the transition zone of rachilla and rachis of control and infected wheat spikelets. Callose plugs in sieve elements of Δ*fgl1-2*-infected spikelets are representative for *P. teres*-induced callose plugs. cd, Callose deposit; se, sieve element; sp, sieve plate. Bars = 20 μm.

callose deposition at the sieve plate, which did not differ compared with controls (Fig. 1D).

During the progress of *F. graminearum* wild type infection, we observed strongest tissue necrosis during *F. graminearum* wild type infection, which affected the complete spike at 14 dpi. We also observed necrotic tissue formation during infection with Δ*fgl1-2*, which started at 7 dpi but only affected the directly inoculated

spikelet at 14 dpi (Fig. 1A). To test whether the observed deposition of additional callose plugs in the phloem of Δ*fgl1-2*- and *P. teres*-infected spikelets is regulated at the transcriptional level, we determined the expression of eight known wheat *GSL* genes (*TaGSL*; Voigt et al., 2006). The results of quantitative real-time PCR revealed that there were no detectable differences in *TaGSL* gene expression in tissues infected with *F. graminearum* wild type, Δ*fgl1-2*, and *P. teres* (Supplemental Fig. S2); therefore, there was no correlation between *TaGSL* gene expression and the observed vascular callose deposition.

Inhibition of Callose Synthase Activity by FFAs

Because we observed a strong repression of pathogen-induced, vascular callose deposition during *F. graminearum* wild type infection but not during Δ*fgl1-2* infection, we proposed that the secreted fungal lipase FGL1 could be involved in the inhibition of callose biosynthesis. To test this, we examined the effect of FFAs on callose synthase activity. Generally, FFAs are products of the hydrolysis of lipids catalyzed by lipases. The callose synthase activity of isolated membranes revealed that the addition of stearic acid (18:0, where *x*:*y* denotes a fatty acid with *x* carbons and *y* double bonds) did not influence callose synthase activity at concentrations ranging from 0.7 to 700 μM (Fig. 2A). Palmitic acid (16:0) inhibited callose synthase activity at concentrations higher than 17.5 μM. However, a strong inhibitory effect was detected for unsaturated FFAs, which inhibited enzyme activity at concentrations of 0.7 and 7 μM, resulting in an 80% reduction of activity at a concentration of 17.5 μM (Fig. 2A). We observed complete inhibition of callose synthase activity due to activity by the polyunsaturated FFAs linoleic acid (18:2) and α-linolenic acid (18:3) at concentrations of 35 μM and higher. The inhibitory effect of the monounsaturated oleic acid (18:1) was not as strong as that of the polyunsaturated FFAs (Fig. 2A). As a positive control, we added the known callose synthase inhibitor 2-deoxy-D-glucose (2-DDG; Bayles et al., 1990) to the activity assay. Compared with the unsaturated FFAs, the inhibitory effect of 2-DDG was even stronger: an 80% reduction of activity was already observed at a concentration of 7 μM and complete inhibition at 17.5 μM (Fig. 2A). To examine whether callose synthase activity would be also inhibited in planta, we applied FFAs and 2-DDG to wheat spikelets. One day after application, the callose synthase activity of directly treated spikelets and adjacent rachis regions resembled the results of the in vitro assay. We only observed a strong inhibition of callose synthase activity for the unsaturated FFAs and 2-DDG, which decreased the activity by 55% to 70% (Fig. 2B).

Unsaturated FFAs Restore Virulence to the Lipase-Deficient *F. graminearum* Mutant Δ*fgl1*

Because unsaturated FFAs were able to inhibit callose synthase activity in planta, we tested whether FFAs may alter the resistance of wheat to *F. graminearum*. The callose synthesis inhibitor 2-DDG and FFAs were applied to spikelets at 3 dpi with the GFP-tagged *F. graminearum* wild-type strain wt-GFP-1 and the lipase-deficient strain Δ*fgl1*-GFP-1 (Supplemental Fig. S3), which allowed monitoring of the infection progress in the wheat spike. In wheat spikes that were infected with Δ*fgl1*-GFP-1, only the addition of unsaturated FFAs and 2-DDG broke the wheat type II resistance to this lipase-deficient strain. We observed an FHB disease phenotype that was similar to wild type-infected spikes mainly above the point of inoculation (Fig. 2C), which reflected the significant increase in the percentage of infected spikelets from about 20% for the Δ*fgl1*-GFP-1 infection without subsequent treatment to about 50% with FFAs and to 70% for 2-DDG treatment at 21 dpi (Table I). In contrast, addition of the saturated FFAs and ethanol as a control did not increase infection severity (Table I) as rated by a colonization scoring system (Supplemental Fig. S4). The addition of ethanol, ethanol-dissolved FFAs, and 2-DDG alone to control spikelets did not result in tissue necrosis or degradation (Table I).

The histological examination of Δ*fgl1*-GFP-1- and wt-GFP-1-inoculated spikelets revealed a similar infection pattern and progress at 1 dpi. Conidia predominantly germinated on pollen-covered stigma of the floret's pistil and fungal hyphae grew in the direction of the ovary (Fig. 2D). At 7 dpi, the effect of unsaturated FFAs and 2-DDG, which were added at 3 dpi when the fungus reached the transition zone of rachilla and rachis (Supplemental Fig. S1), on the infection severity of the lipase-deficient Δ*fgl1*-GFP-1 strain was clearly detectable. Whereas the infection of Δ*fgl1*-GFP-1 without supplementation was restricted to the inoculated spikelet with only single hyphae in the adjacent rachis, the application of callose synthase inhibitors restored virulence to the Δ*fgl1*-GFP-1 strain and broke the previously observed type II resistance of the wheat spike to this lipase-deficient fungal mutant. Δ*fgl1*-GFP-1 supplemented with either unsaturated FFAs or 2-DDG repressed pathogen-induced, vascular callose deposition (Fig. 2E) and crossed the transition zone of the rachilla and rachis and colonized the adjacent rachis region (Fig. 2F; Supplemental Fig. S5). The colonization severity of the transition zone of rachilla and rachis by the Δ*fgl1* strain supplemented with either α-linolenic acid or 2-DDG was similar to *F. graminearum* wild type and stronger than Δ*fgl1* without supplementation at 7 dpi (Figs. 1A and 2F; Supplemental Fig. S5). However, the macroscopic FHB disease phenotype at 21 dpi (Fig. 2C) as well as the statistical analysis of rachis colonization severity (Table I) indicated that the addition of unsaturated FFAs or 2-DDG did not completely restore virulence to the lipase-deficient Δ*fgl1* strain. Therefore, we performed a histological analysis of wheat spike tissue colonization at 14 dpi. As expected, colonization of the lipase-deficient Δ*fgl1-2* strain was restricted to the transition zone of the rachilla and rachis of directly inoculated spikelets. In contrast, *F. graminearum* wild type also colonized wheat spike tissue above and below the inoculated spikelets by growing through the rachis (Fig.

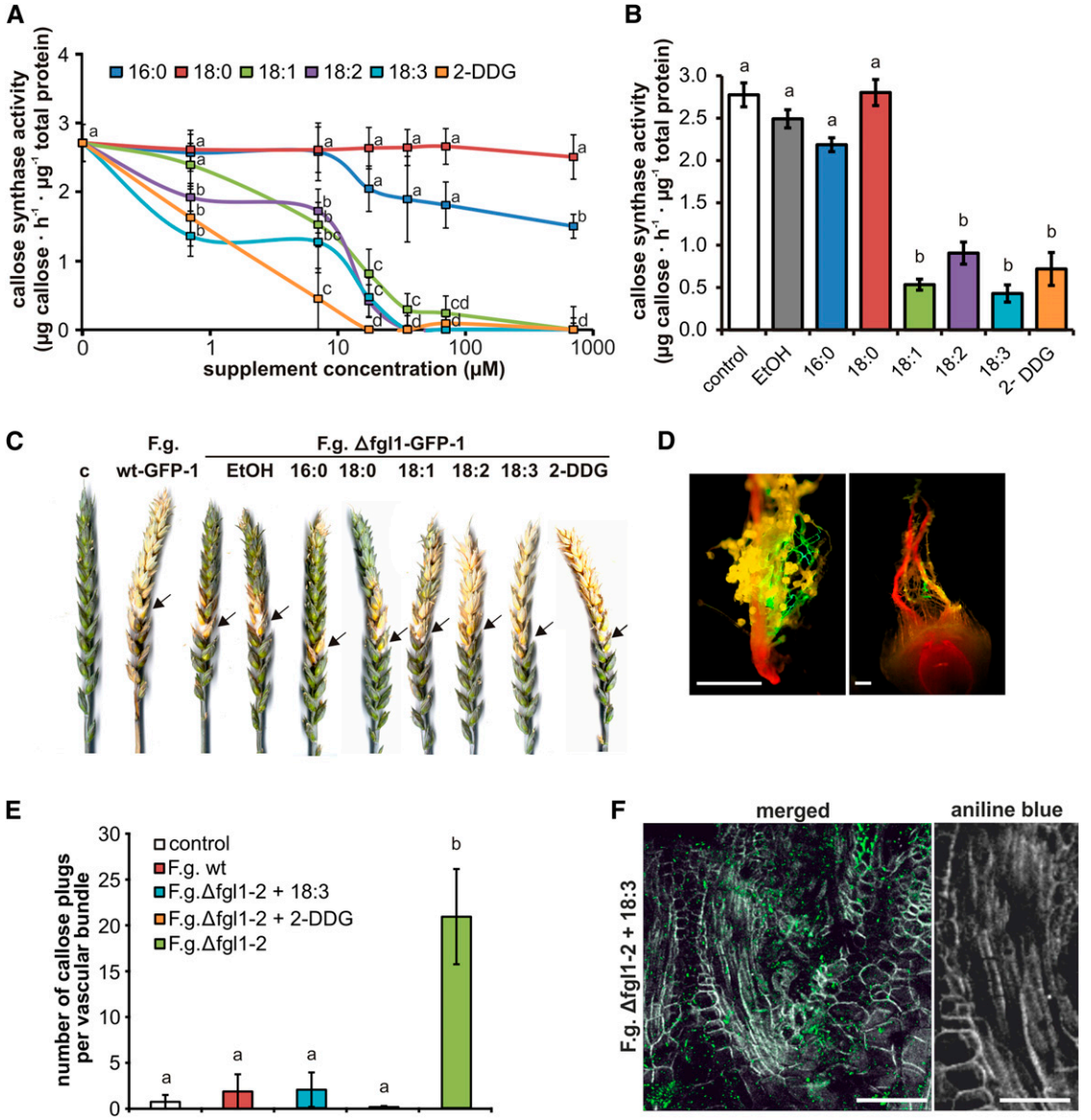

Figure 2. FFA and 2-DDG impact on callose biosynthesis and disease phenotypes of *F. graminearum*-infected wheat spikes. A, Callose synthase activity of membranes isolated from untreated wheat spikes at Zadoks stages 7.5 to 7.9 (Zadoks et al., 1974). Ethanol-dissolved FFAs and the callose synthesis inhibitor 2-DDG were added to membrane preparations at the final concentrations indicated. FFAs were palmitic acid (16:0), stearic acid (18:0), oleic acid (18:1), linoleic acid (18:2), and α-linolenic acid (18:3). B, Callose synthase activity of membranes isolated from spikelets and the adjacent rachis region 24 h after FFA and 2-DDG application. Four microliters of ethanol-dissolved FFAs or 2-DDG (concentration, 3.2 mM) and pure ethanol (EtOH) was added to wheat spikelets at Zadoks stages 7.02 to 7.05 (Zadoks et al., 1974). For A and B, values represent means of two biologically independent experiments. The letters a to d indicate $P < 0.05$ by Tukey's test. Error bars represent SE, and $n = 6$. C, Inoculation of two central spikelets with 10 μL of water (control [C]) and *F. graminearum* strains wt-GFP-1 and Δ*fgl1*-GFP-1. Four microliters of ethanol-dissolved FFAs and 2-DDG (concentration, 3.2 mM) and pure ethanol was added to each of the previously inoculated spikelets at 3 dpi. Arrows indicate the inoculation sites. Pathogenicity tests were repeated 10 times for strain wt-GFP-1 and 20 times for strain Δ*fgl1*-GFP-1. Spikes are representative for infection severity at 21 dpi. wt-GFP-1 inoculation is representative for infection with or without the addition of FFAs or 2-DDG (Table I). D, Micrographs of isolated stigma and pistil from a floret at 1 dpi. Hyphal growth was directed from pollen on stigmas toward the ovary. No differences were seen between wt-GFP-1 and Δ*fgl1*-GFP-1 growth at 1 dpi. Bars = 40 μm. E, Number of callose plugs located in phloem of the vascular bundles of the transition zone of rachilla and rachis tissue from spikelets directly inoculated with Δ*fgl1-2* supplemented (as described in C) with either α-linolenic acid (F.g. Δfgl1-2 + 18:3) or 2-DDG (F.g. Δfgl1-2 + 2-DDG) at 7 dpi, including data from an analysis of *F. graminearum* wild type (F.g. wt), lipase-deficient strain Δ*fgl1-2* without supplementation, and the control (Fig. 1C). Values represent means of eight biologically independent inoculation experiments for each fungal strain. The letters a and b indicate $P < 0.05$ by Tukey's test. Error bars represent SE, and $n = 8$. F, Section of a directly inoculated

3A). We observed a similar colonization severity for Δ*fgl1-2* supplemented with either α-linolenic acid or 2-DDG in wheat spike tissue at the site of inoculation and above the inoculated spikelets (Supplemental Fig. S6). Colonization severity of the rachis below the inoculated spikelets was reduced compared with *F. graminearum* wild type (Fig. 3A). The addition of FFAs and 2-DDG to *F. graminearum* wild type did not change the overall strength of infection at 7, 14, or 21 dpi (Table I; Supplemental Fig. S7). To exclude a nutritional effect of the added long-chain, polyunsaturated FFAs or 2-DDG on *F. graminearum* growth, which might support partial complementation of the lipase-deficient Δ*fgl1* strain, we tested fungal growth on supplemented minimal medium. Plate growth assays revealed that none of the tested FFAs or 2-DDG promoted fungal growth (Supplemental Fig. S8).

We then determined the concentration of the mycotoxin deoxynivalenol (DON), a major virulence factor of *F. graminearum* (Proctor et al., 1995), in three different wheat spike sections to evaluate the observed differences in the severity of fungal tissue colonization. DON concentration was highest in directly inoculated spikelet tissue without significant differences between *F. graminearum* wild type and the lipase-deficient strain Δ*fgl1-2* with and without α-linolenic acid or 2-DDG supplementation at 7 dpi as well as 14 dpi (Fig. 3B). These DON concentrations resembled the strong colonization severity of inoculated spikelets at the examined time points (Figs. 1A, 2F, and 3A). We also found a strong correlation between colonization severity and DON concentration for wheat spike tissue above and below the inoculation site for *F. graminearum* wild type and Δ*fgl1-2* without supplementation, where strong colonization severity resulted in high DON concentrations and failure to colonize wheat tissue in the absence of DON (Fig. 3). This correlation was broken for Δ*fgl1-2* supplemented with either α-linolenic acid or 2-DDG, where we detected a similar colonization severity of the tissue above the inoculation site as for *F. graminearum* wild type infection but a strongly reduced DON concentration at 14 dpi (Fig. 3). Because we found localized callose plugs in the vascular bundles of Δ*fgl1-2*-infected wheat spikelets and a relatively high DON concentration in the same tissue at 7 dpi (Figs. 1, A and C, and 3B), we concluded that DON might not be required to suppress vascular callose deposition. To test this, we inoculated the wheat spike with the DON-deficient Δ*tri5* mutant, obtained by disrupting the trichodiene synthase encoding gene *Tri5* (Jansen et al., 2005), which resulted in colonization of the spikelet's transition zone of rachilla and rachis (Supplemental Fig. S9A) without the formation of callose plugs within the vascular tissue (Supplemental Fig. S9B).

To further evaluate the observed differences in the severity of fungal tissue colonization and a putative effect of FFAs on plant signal transduction (Bai and Shaner, 1994; Baudouin et al., 1999; Jones and Dangl, 2006), we determined the expression of five pathogenesis-related genes of wheat (*TaPR1–TaPR5*) in quantitative real-time PCR assays at 7 dpi (Supplemental Fig. S10). Spikelets were inoculated with *F. graminearum* wild type and the lipase-deficient strain Δ*fgl1-2* without and with the addition of the callose synthesis inhibitor α-linolenic acid or 2-DDG. Similar to DON concentrations, we observed a strong correlation between colonization severity and the induction of *TaPR* gene expression after infection with *F. graminearum* wild type and Δ*fgl1-2* without supplementation. Whereas the expression of all five *TaPR* genes in all three examined wheat spike sections was strongest after *F. graminearum* wild type infection, a relatively strong induction of gene expression after Δ*fgl1-2* infection was restricted to *TaPR1* and *TaPR3* in directly inoculated spikelets (Supplemental Fig. S10). Infection with Δ*fgl1-2* supplemented with 2-DDG induced a similar *TaPR* gene expression in wheat spike tissue of the inoculation site and the spike section above to *F. graminearum* wild type infection, but it was strongly reduced in the wheat spike section below the inoculation site (Supplemental Fig. S10). Comparing *TaPR* gene expression after infection with Δ*fgl1-2* supplemented with either α-linolenic acid or 2-DDG, we observed main differences in *TaPR1* and *TaPR3* expression at the site of inoculation and the section above, where the induction of gene expression was significantly lower after infection with Δ*fgl1-2* supplemented with α-linolenic acid (Supplemental Fig. S10).

FFA Concentrations in Wheat Spikelets after Lipase Application and during Infection

Because unsaturated FFAs inhibited callose biosynthesis in planta and partially restored virulence to the Δ*fgl1* strain, we tested whether the secreted *F. graminearum* lipase FGL1 would be capable of releasing the respective FFAs from wheat spike tissue. We applied 1.3 units of purified FGL1, which was heterologously expressed in *Pichia pastoris* (Supplemental Fig. S11), to single, untreated spikelets. Sixteen hours after lipase application, we observed only single spots of degraded and necrotic tissue at the floret's lemma, but the ovary turned completely brownish and showed symptoms of degradation (Supplemental Fig. S12). The determination of the FFA concentration in the FGL1-treated

Figure 2. (*Continued.*)
wheat spikelet comprising the transition zone of rachilla and rachis including vascular bundles at 7 dpi with Δ*fgl1-2* supplemented with α-linolenic acid. Micrographs were taken by confocal laser-scanning microscopy. Green color was assigned to fungal hyphae stained with Alexa Fluor 488-conjugated wheat germ agglutinin, and grayscale was assigned to aniline blue-stained callose. Micrographs are representative for infection at 7 dpi. Bars = 200 μm (left) and 100 μm (right).

Table I. *Differences in virulence of GFP-tagged F. graminearum strains to wheat due to the application of FFAs and 2-DDG*

Wheat spikelets were inoculated with 400 conidia of *F. graminearum* wt-GFP-1 and Δfgl1-GFP-1. Four microliters of ethanol-dissolved FFAs and 2-DDG (concentration, 3.2 mM) and ethanol as a control was added at 3 dpi to each of the previously inoculated spikelets. FFAs were palmitic acid (16:0), stearic acid (18:0), oleic acid (18:1), linoleic acid (18:2), and α-linolenic acid (18:3).

Treatment[a]	Percentage of Infection[b]		Percentage of Rachis Colonization[c]	Rating of Rachis Colonization Severity[d]	
	Mean	SE		Mean	SE
Ethanol control	0.0	–	–	–	–
16:0 control	0.0	–	–	–	–
18:0 control	0.0	–	–	–	–
18:1 control	0.0	–	–	–	–
18:2 control	0.0	–	–	–	–
18:3 control	0.0	–	–	–	–
2-DDG control	0.0	–	–	–	–
wt-GFP-1	80.5	8.7[e]	100	2.7	0.2[e]
wt-GFP-1 + ethanol	88.2	5.4[e]	100	2.9	0.1[e]
wt-GFP-1 + 16:0	84.4	7.6[e]	100	2.5	0.3[e]
wt-GFP-1 + 18:0	86.5	4.6[e]	100	2.8	0.1[e]
wt-GFP-1 + 18:1	84.9	4.8[e]	100	2.8	0.1[e]
wt-GFP-1 + 18:2	82.8	4.9[e]	100	2.9	0.1[e]
wt-GFP-1 + 18:3	81.5	4.9[e]	100	2.9	0.1[e]
wt-GFP-1 + 2-DDG	84.5	6.1[e]	100	2.6	0.2[e]
Δfgl1-GFP-1	22.1	5.3[f]	45.0	0.7	0.2[f]
Δfgl1-GFP-1 + ethanol	20.5	4.2[f]	39.1	0.5	0.2[f]
Δfgl1-GFP-1 + 16:0	18.7	2.7[f]	25.0	0.3	0.1[f]
Δfgl1-GFP-1 + 18:0	31.2	5.2[f]	60.0	1.1	0.3[g]
Δfgl1-GFP-1 + 18:1	51.2	6.3[h]	73.7	1.6	0.3[h]
Δfgl1-GFP-1 + 18:2	51.8	5.9[h]	90.0	2.0	0.2[h]
Δfgl1-GFP-1 + 18:3	49.6	6.8[h]	85.0	1.9	0.2[h]
Δfgl1-GFP-1 + 2-DDG	70.8	8.0[h]	80.0	1.9	0.2[h]

[a]Repeat experiments gave similar results. [b]Infection referred to partially or completely bleached spikelets observed at 21 dpi. Spikelets with minor symptoms (tiny yellow or brown spots) were not counted. Results are averages of 10 (control and wt-GFP-1) and 20 (Δfgl1-GFP-1) wheat spikes (16–24 spikelets per spike). [c]Percentage of all inoculations with GFP-tagged *F. graminearum* mycelium detectable in rachis tissue located between two inoculated spikelets. [d]Colonization severity by rating the green fluorescence of GFP-tagged *F. graminearum* mycelium in rachis tissue located between two inoculated spikelets at 21 dpi (Supplemental Fig. S3). Results are averages of 10 (wt-GFP-1) and 20 (Δfgl1-GFP-1) inoculated wheat spikes. [e]Statistically different from Δfgl1-GFP-1 strains with or without the addition of FFAs or 2-DDG, with no statistical differences among approaches ($P < 0.05$). [f]Statistically different from Δfgl1-GFP-1 strains with the addition of unsaturated FFAs and 2-DDG, with no statistical differences among approaches ($P < 0.05$). [g]Rachis colonization severity was not statistically different from that of Δfgl1-GFP-1 strains with the addition of other FFAs or without the addition of FFAs ($P < 0.05$). [h]No statistical differences among approaches ($P < 0.05$).

spikelet tissue revealed highest values for palmitic (16:0), linoleic (18:2), and α-linolenic (18:3) acids, where we observed a constant increase in FFA concentration between 0.5 and 16 h after lipase application (Fig. 4A). FGL1 also released stearic acid (18:0) and oleic acid (18:1) from the spikelet tissue; however, the concentrations were relatively low (Fig. 4A). Based on the results of FGL1-dependent lipid hydrolysis within the wheat spikelet, we anticipated higher concentrations of linoleic acid (18:2) and α-linolenic acid (18:3) during *F. graminearum* wild type than Δ*fgl1* infection. These two polyunsaturated FFAs fulfilled the prerequisites of effective callose synthesis inhibitors, because our previous callose synthase activity assay showed that inhibition of enzymatic activity was dependent on the structure and the concentration of the inhibiting FFAs (Fig. 2A). The results of the FFA measurement confirmed this hypothesis. Especially the combination of linoleic acid (18:2) and α-linolenic acid (18:3), both with the highest inhibition of callose synthase activity (Fig. 2, A and B), revealed a significantly higher FFA quantity in *F. graminearum* wild type-infected than Δ*fgl1*-infected and control tissues. At 5 dpi, the FFA quantity was about 90% higher after wild type infection compared with control tissue and about 50% higher than in Δ*fgl1*-infected spikelets (Fig. 4B). The combined amount of linoleic acid (18:2) and α-linolenic acid (18:3) further increased during infection and was almost 160% higher in wild type-infected than control spikelets and still 40% higher than in Δ*fgl1*-infected spikelets at 7 dpi (Fig. 4B). Palmitic acid (16:0) was significantly higher in infected tissues at 7 dpi compared with control tissue (Fig. 4B). However, this FFA neither inhibited callose biosynthesis in planta (Fig. 3B) nor restored virulence to the lipase-deficient *F. graminearum* strain (Table I). The quantification of the corresponding esterified fatty acids did not show significant differences between *F. graminearum* wild type-infected, Δ*fgl1*-infected, or control samples, and the concentration of each esterified fatty acid also remained stable (Supplemental Table S1).

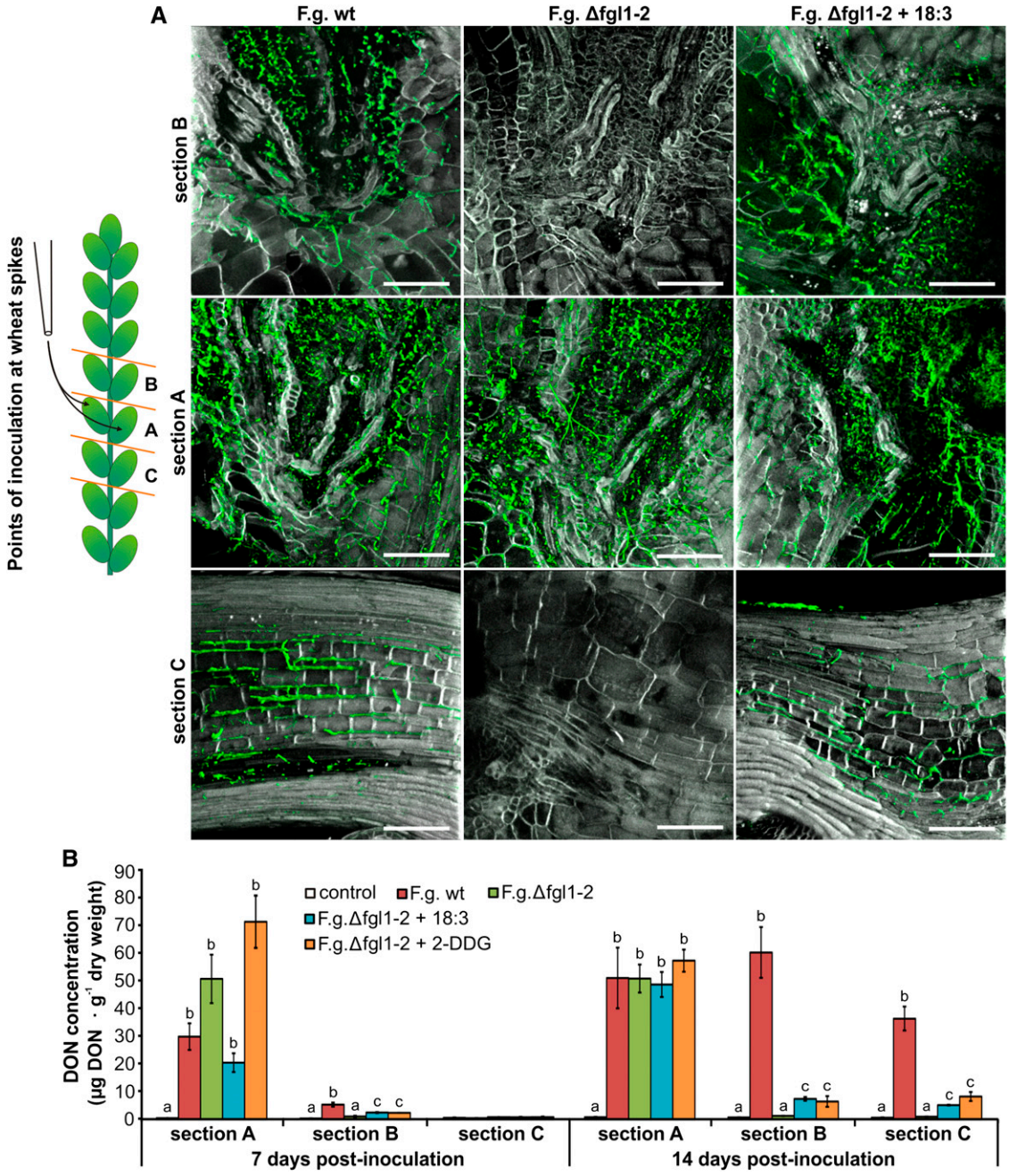

Figure 3. FFA and 2-DDG impact on the progress of *F. graminearum* infection and mycotoxin production in wheat spikes. A, Sections of directly inoculated spikelets comprising the transition zone of rachilla and rachis (section A), the transition zone of rachilla and rachis of spikelets above inoculated spikelets (section B), and the rachis region below inoculated spikelets (section C). Inoculation was with *F. graminearum* wild type (F.g. wt), lipase-deficient strain Δ*fgl1-2* (F.g. Δfgl1-2), and Δ*fgl1-2* supplemented with α-linolenic acid (F.g. Δfgl1-2 + 18:3). Supplementation was by the addition of 4 μL of ethanol-dissolved 18:3 (concentration, 3.2 mM) to each of the previously inoculated spikelets at 3 dpi. Micrographs were taken by confocal laser-scanning microscopy at 14 dpi. Green color was assigned to fungal hyphae stained with Alexa Fluor 488-conjugated wheat germ agglutinin, and grayscale was assigned to aniline blue-stained callose. Micrographs are representative for the infection progress in spikelets inoculated with *F. graminearum* wild type (no differences with or without the addition of FFAs or 2-DDG) and lipase-deficient strain Δ*fgl1-2*. Changes in infection progress due to the addition of unsaturated FFAs or 2-DDG to Δ*fgl1-2*-infected spikelets are represented by images of infection after the addition of 18:3. Bars = 200 μm. B, DON concentrations of wheat spike tissue from sections A, B, and C (compare the schematic overview in A) at 7 and 14 dpi with *F. graminearum* wild type, lipase-deficient strain Δ*fgl1-2*, and Δ*fgl1-2* supplemented with α-linolenic acid or 2-DDG. Values represent means of two biologically independent experiments. The letters a, b, and c indicate $P < 0.05$ by Tukey's test. Error bars represent SE, and $n = 3$.

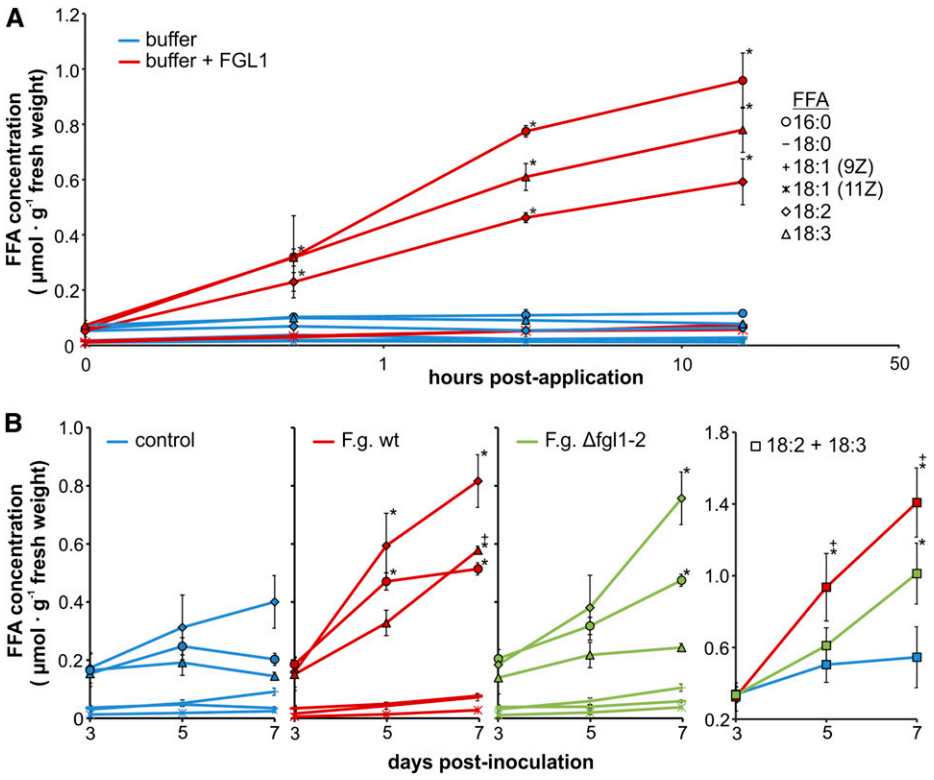

Figure 4. FFA concentrations in wheat spikes after lipase application and *F. graminearum* infection. A, FFA concentrations in wheat spikelets after application of the purified *F. graminearum* effector lipase FGL1. Untreated spikelets served as controls. Samples were taken at 0, 0.5, 3, and 16 h after application. FFAs were palmitic acid (16:0), stearic acid (18:0), oleic acid (18:1), linoleic acid (18:2), and α-linolenic acid (18:3). B, FFA concentrations in wheat spikelets inoculated with *F. graminearum* wild type (F.g. wt) and the lipase-deficient mutant Δ*fgl1-2* (F.g. Δfgl1-2). Uninfected spikelets served as controls. Samples were taken at 3, 5, and 7 dpi. Values represent means of two biologically independent experiments. *Statistically different from the control; †statistically different from Δ*fgl1-2* at $P < 0.05$ by Tukey's test. Error bars represent SE, and $n = 6$.

Likewise, the corresponding free and esterified oxylipins also did not differ in infected or control wheat spikelet tissue (Supplemental Table S1). We also excluded a nutritional effect of altered FFA amounts on *F. graminearum* growth, because we did not observe differences in the relative *F. graminearum* mycelium amount comparing wild type- and Δ*fgl1*-infected spikelet tissue (Supplemental Table S2).

DISCUSSION AND CONCLUSION

Our histological analysis of the wheat spikelet's transition zone of rachilla and rachis revealed that the effective type II resistance to the *F. graminearum* mutant Δ*fgl1*, disrupted in the production of the effector lipase FGL1 (Voigt et al., 2005), and the nonadapted barley leaf pathogen *P. teres* was associated with a strong callose deposition in sieve elements of the spikelet's phloem. An increased callose deposition in the spikelet's transition zone in combination with type II resistance was also reported for the wheat cv Sumai 3 (Ribichich et al., 2000), where the spreading of *F. graminearum* was strongly reduced compared with a susceptible wheat cultivar. The deposition of callose in the phloem also occurred after bacterial infection of *Citrus* spp. leaves, where callose plugged sieve pores, probably to inhibit phloem transport (Koh et al., 2012). In contrast to the lipase-deficient mutant Δ*fgl1* and *P. teres*, *F. graminearum* wild type inhibited callose deposition in the phloem of the spikelet, putatively through the suppression of callose biosynthesis. Based on the results of the expression of eight known wheat *GSL* genes (Voigt et al., 2006) during infection of the wheat spike, we also excluded the regulation of callose biosynthesis through the alteration of transcriptional levels of callose synthase-encoding genes. Even though the regulation of *TaGSL* genes occurred at the transcriptional level, none of the expression patterns correlated with the stress-induced regulation of callose synthase activity. This supports the idea of a subcellular control of preexisting enzymes, as proposed by Jacobs et al. (2003) and as recently shown in our study, where we overexpressed the stressed-induced callose synthase gene *AtGSL5* in Arabidopsis (Ellinger et al., 2013). Hence, we anticipated an involvement of the secreted effector lipase FGL1 in the suppression of callose biosynthesis.

A link between the lipase FGL1 and the inhibition of callose biosynthesis was given in a study with soybean (*Glycine max*), where FFAs inhibited callose synthase activity in in vitro assays (Kauss and Jeblick, 1986). Because lipid hydrolysis by lipases generally releases FFAs and the lipid backbone (e.g. glycerol or lyso lipids), we tested the major fatty acids occurring in wheat (Davis et al., 1980; Barnes, 1982) for their ability to inhibit wheat callose biosynthesis. The determination of callose synthase activity revealed that the unsaturated FFAs oleic (18:1), linoleic (18:2), and α-linolenic (18:3) acids inhibited callose synthesis in in vitro as well as in planta assays at similar concentrations to those reported for soybean (Kauss and Jeblick, 1986). Moreover, the FFA concentrations were below the critical micelle concentration (Verhagen et al., 1978; Murakami et al., 1986; Sellhorn

et al., 2011), which may suggest that the biological activity of the FFAs was based on the free molecules and their direct interaction with the enzyme. Alternatively, the liberated FFAs may stay in the membrane. This may lead to an alteration of the physicochemical properties and thereby regulate the activity of the membrane (associated) protein callose synthase. The addition of the unsaturated FFAs to wheat spikelets that were previously inoculated with the Δ*fgl1* strain partially restored virulence by breaking the type II resistance, which was associated with the suppression of callose deposition in the vascular tissue. Interestingly, we observed a first indication of an active suppression of callose biosynthesis at 3 dpi, when callose deposition started to occur in the phloem of spikelets inoculated with the lipase-deficient Δ*fgl1* strain but not in *F. graminearum* wild type-infected spikelets. This coincided with the induction of *FGL1* gene expression during wheat spike infection, where expression peaked at 7 dpi (Voigt et al., 2005). At the same time, we detected a higher combined linoleic and α-linolenic acid concentration in wheat spikelets at 5 and 7 dpi with *F. graminearum* wild type than in Δ*fgl1*-infected and control spikelets.

Apart from linoleic and α-linolenic acids, also oleic acid showed a similar capacity in inhibiting callose biosynthesis and restoring virulence to the Δ*fgl1* strain. However, the contribution of saturated palmitic acid to callose biosynthesis inhibition is likely to be negligible. This is because palmitic acid did not inhibit callose biosynthesis in planta, despite the relatively large quantities released after FGL1 treatment and during infection. These findings support our hypothesis of plant defense suppression by the inhibition of callose biosynthesis through FGL1-dependent release of unsaturated FFAs. In this model, the inhibition of callose biosynthesis would then prevent localized, pathogen-induced callose deposition in sieve elements of the phloem; this inhibition may be essential to break a component of the spikelet's type II resistance (Fig. 5). In addition to acting as a physical barrier by strengthening the plant cell well, callose deposition may also plug sieve elements (Stone and Clarke, 1992; Koh et al., 2012; Ellinger et al., 2013). Unplugged phloem may not only ease fungal colonization and spreading but also allow the dissemination through the vascular system of mycotoxins (including DON, a major virulence factor of *F. graminearum*; Kang and Buchenauer, 1999) and of secreted effector proteins (Brown et al., 2012) ahead of *F. graminearum* colonization. However, this may not affect the salicylic acid or α-linolenic acid-dependent jasmonic acid pathway, both known to be involved in plant defense (Kouker and Jaeger, 1987; Brown et al., 1998; Schwessinger and Ronald, 2012). Even though salicylic acid and jasmonic acid levels generally increased during infection, we did not observe a difference between *F. graminearum* wild type and Δ*fgl1* infection. Moreover, we did not detect differences in the other oxylipins we analyzed in this study (Supplemental Table S1).

Apart from suppressing callose biosynthesis, the lipase FGL1 might also be involved in DON induction outside the directly inoculated spikelet. Despite a similar severity of tissue colonization above the site of inoculation, we determined a strong reduction of the DON amount in the spike tissue infected by Δ*fgl1* after α-linolenic acid or 2-DDG complementation compared

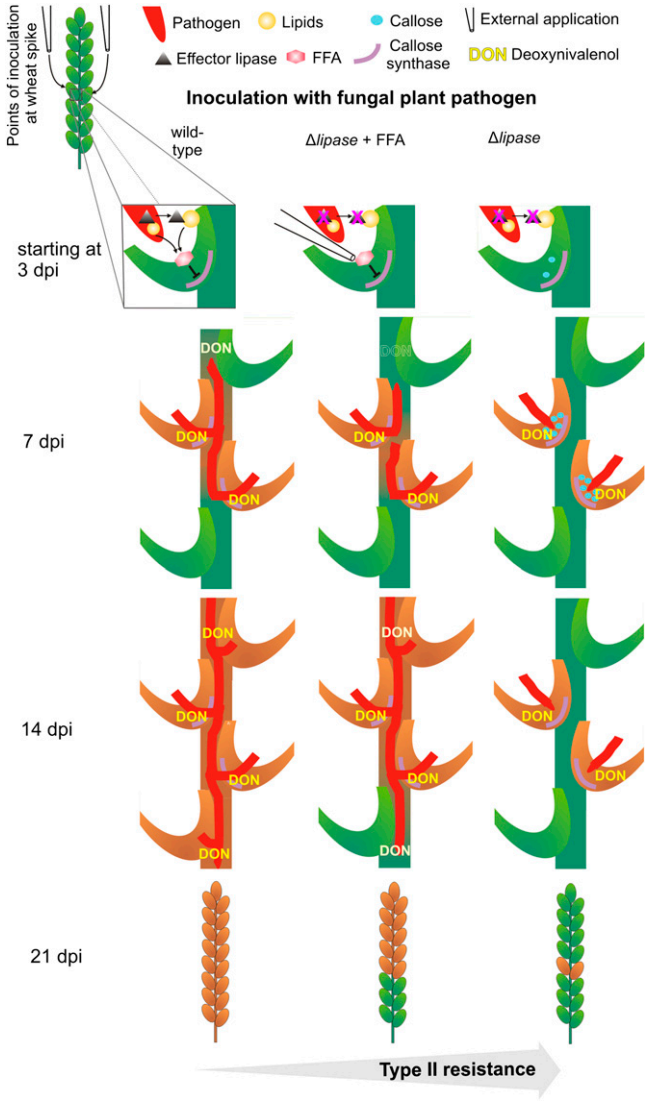

Figure 5. Effector lipase-dependent type II resistance to fungal infection in wheat. The model shows the determination of type II resistance to fungal infection in wheat based on our results of pathogen-caused suppression of the plant defense-related callose formation. Left, susceptible wheat characterized by callose synthases that are strongly inhibited by polyunsaturated FFAs due to pathogen-derived effector lipase activity; middle, application of polyunsaturated FFAs (partially) restores the virulence of lipase-deficient fungal pathogen unable to release FFAs due to missing lipase; right, lipase-deficient fungal pathogen (or incompatible pathogen) without release of FFAs due to missing lipase. Pathogen-induced callose formation is not inhibited and promotes type II resistance in planta.

with *F. graminearum* wild type infection. The lack of mycotoxin induction in the Δ*fgl1* strain outside the directly inoculated spikelet might explain why supplementation with callose biosynthesis inhibitors is sufficient to break the type II resistance barrier within the inoculated spikelet while it does not restore complete virulence. Interestingly, a wild-type-like DON production within the inoculated spikelet is not sufficient to break the spikelet's type II resistance if a callose biosynthesis inhibitor is missing, as revealed in the disease phenotype of the DON-producing Δ*fgl1* mutant. On the other hand, the DON-deficient *F. graminearum* Δ*tri5* mutant, which, like all other DON-deficient mutants, phenotypically elicits the same strong type II resistance reaction in wheat plants (Proctor et al., 1995; Desjardins et al., 1996; Bai et al., 2002; Voigt et al., 2005), was able to suppress localized callose deposition but failed to colonize the spike's rachis due to the missing mycotoxin DON. This not only shows that the mycotoxin DON is not required to inhibit callose biosynthesis but also highlights the multilayered character of type II resistance in the wheat spikelet.

From our results, we conclude that the inhibition of callose synthesis is mainly based on the pathogen-caused release of linoleic and α-linolenic acids. However, we have not yet identified the lipid source of the released unsaturated FFAs in the pathosystem wheat-*F. graminearum*. The observed infection process and the physiology of the infected plant organs suggest a plant lipid as the source for pathogen-caused hydrolysis. The growth of *F. graminearum* conidia after germination was directed to the ovary of the floret, similar to the growth behavior of *Fusarium culmorum* in inoculated wheat spikes (Kang and Buchenauer, 2000). The pistil is enriched in nutrients and lipids. Furthermore, it is adjacent to the transition zone of rachilla and rachis, where we observed induced callose deposition in the vascular tissue after Δ*fgl1* infection. Hence, the combination of lipids and the position of the pistil's ovary could enable the inhibition of callose synthases due to lipid hydrolysis in the region of the rachis node. Although unsaturated FFAs might also be derived from the hydrolysis of *F. graminearum* lipids, which also contain the polyunsaturated linoleic and α-linolenic acids (Guenther et al., 2009), we would not expect a major contribution from fungal lipids, because *F. graminearum* mycelium contains a maximum of 7.5% lipids (Guenther et al., 2009) and accounted for 0.1% of the combined fungal and plant biomass (Supplemental Table S2).

We suggest that an early, enhanced callose deposition in the phloem of the transition zone of rachilla and rachis before the FGL1-mediated suppression of callose synthesis starts at 3 dpi might be effective to stop or delay fungal spreading and to prevent or reduce FHB. This could be achieved through the overexpression of those callose synthases that are involved in pathogen-induced callose deposition, a strategy that we successfully applied in Arabidopsis to prevent powdery mildew infection (Ellinger et al., 2013).

MATERIALS AND METHODS

Fungal Strains and Culture Conditions

Fusarium graminearum strain 8/1 was obtained from Thomas Miedaner (Miedaner et al., 2000). Lipase-deficient *F. graminearum* strain Δ*fgl1-2* and DON-deficient *F. graminearum* strain Δ*tri5* were derived from our previous studies (Jansen et al., 2005; Voigt et al., 2005). Media, culture conditions, and induction of conidiation were according to Voigt et al. (2005). *Pyrenophora teres* strain 15A was provided by Brian J. Steffenson (Weiland et al., 1999). Culture conditions and induction of conidia were according to Ruiz-Roldán et al. (2001).

Plant Inoculation and Pathogenicity Tests on Wheat

Wheat (*Triticum aestivum* 'Nandu'; Lochow-Petkus) was cultivated and inoculated as described by Voigt et al. (2005). Inoculation of two central spikelets was performed with conidia of *F. graminearum* wild type, Δ*fgl1-2*, GFP-tagged *F. graminearum* strains wt-GFP-1 and Δ*fgl1*-GFP-1 (Supplemental Fig. S1), and *P. teres* wild type. The effect of the *F. graminearum* lipase FGL1 on tissue degradation and lipid hydrolysis was tested by applying 10 μL of FGL1 solution (activity, 1.3 units) to untreated spikelets at Zadoks stages 7.5 to 7.9 (Zadoks et al., 1974).

Addition of FFAs and 2-DDG to Infected Wheat Plants

To detect an impact of FFAs and the callose inhibitor 2-DDG on the resistance of wheat to *F. graminearum* infection, 2 μL of ethanol-dissolved FFAs, 2-DDG (both at a concentration of 3.2 mM), and pure ethanol as a control was added to each of the florets at 3 dpi with *F. graminearum* wt-GFP-1 and Δ*fgl1*-GFP-1.

Microscopic Analyses

For confocal laser-scanning microscopy, sections of the wheat spike were destained in 95% ethanol and subsequently costained with aniline blue to localize callose depositions and Alexa Fluor 488-conjugated wheat germ agglutinin (Life Technologies) for selective labeling of fungal hyphae (Meyberg, 1988). Stained sections were mounted between a microscope slide and coverslip in water. Images were captured using the LSM 780 confocal laser-scanning microscope (Zeiss) with a Zeiss Plan-Neofluar 10× objective or with a Zeiss 63× C-Apochromat water-immersion objective for high-resolution microscopy. Aniline blue was excited at 405 nm by using a diode laser; Alexa Fluor 488-conjugated wheat germ agglutinin was excited at 488 nm by using an argon laser. Emission filtering was achieved using a 475- to 495-nm bandpass filter for aniline blue and a 512- to 532-nm bandpass filter. Image processing to obtain a maximum intensity projection was performed using integral functions of the ZEN 2010 (Zeiss) operating software.

For epifluorescence microscopy of freshly cut wheat spikes inoculated with *F. graminearum* wt-GFP-1 and Δ*fgl1*-GFP-1, the stereo fluorescence microscope Leica MZ FLIII (Wetzlar) with the Leica GFP2 filter set (excitations, 480/40 nm; barrier filter, 510 nm) was used.

Membrane Preparation, Callose Synthase Activity Assay, Callose Determination, and FFA Treatment

All procedures for membrane preparation, callose synthase activity assay, and callose determination were performed as described by Voigt et al. (2006). A possible impact of FFAs on wheat callose synthase activity was examined by preparing membranes from untreated spikes at Zadoks stages 7.5 to 7.9 (Zadoks et al., 1974), which represent defined growth stages in the decimal code system of Zadoks for optimal point inoculation of spikelets with *F. graminearum*. Reaction wells of microtiter plates were supplemented with 2 μL of ethanol-dissolved FFAs or 2-DDG, giving final concentrations of 0.7, 7, 17.5, 35, 70, and 700 μM, and pure ethanol as a control. FFAs were palmitic acid (16:0; Merck), stearic acid (18:0; Merck), oleic acid (18:1; Sigma), linoleic acid (18:2; Sigma), and α-linolenic acid (18:3; Sigma); 2-DDG was from Sigma.

To examine the inhibitory effect of FFAs and 2-DDG in planta, six wheat spikelets per spike were each treated with 4 μL of ethanol-dissolved FFAs or 2-DDG (concentration, 3.2 mM) and pure ethanol as a control at Zadoks stages 7.02 to 7.05 (Zadoks et al., 1974). These growth stages were chosen to ensure a

similar growth stage at the time point of sample collection 24 h after FFA or 2-DDG application, as in the experimental setups described above (Zadoks stages 7.5 to 7.9). Samples of five independently treated spikes were pooled. Membranes were prepared from directly inoculated spikelets and the adjacent rachis region. Callose synthase activity was measured as described above.

DON Determination

To determine the concentration of the mycotoxin DON in *F. graminearum*-infected wheat spikes, freshly ground tissue samples were lyophilized. Samples of 10 mg of lyophilized tissue were used in the Ridascreen DON assay (R-Biopharm) according to the manufacturer's instructions.

Fatty Acid Determination

Fatty acids and oxylipins were analyzed as described by Göbel et al. (2003) with some modifications. One gram of frozen wheat spike tissue at 0, 0.5, 3, and 16 h after FGL1 application and at 0, 3, 5, and 7 dpi with *F. graminearum* wild type and Δ*fgl1-2* and the respective controls was extracted by adding 10 mL of extraction medium and homogenized as described by Göbel et al. (2003). Prior to extraction, a mixture of internal standards was added: 50 μg of heptadecanoic acid, 100 ng of D_6-jasmonic acid and 100 ng of D_5-oxophytodienoic acid (both kindly provided by Otto Miersch), plus 13γ-hydroxy octadecatrienoic acid. The extract was shaken for 10 min and centrifuged at 3,200*g* at 4°C for 10 min. The upper phase was collected. A 6.7% (w/v) potassium sulfate solution was added up to a volume of 32.5 mL. After shaking and centrifugation at 3,200*g* at 4°C for 10 min, the upper hexane-rich layer was dried under streaming nitrogen. The remaining lipids were redissolved in 0.2 mL of methanol. For the analysis of FFAs, 20 μL of the sample was methylated after the addition of 380 μL of methanol and 6.5 μL of trimethylsilyldiazomethane (2 M in hexane; Sigma). After shaking for 30 min, 0.2 μL of glacial acetic acid was added. The corresponding fatty acid methyl esters were dried under streaming nitrogen and redissolved in 20 μL of acetonitrile. The fatty acid methyl esters were analyzed with an Agilent 6890 gas chromatograph fitted with a capillary DB-23 column (30 m × 0.25 mm, 0.25 μm coating thickness; J&W Scientific, Agilent). The carrier gas was helium (1 mL min^{-1}). The temperature gradient was 150°C for 1 min, 150°C to 200°C at 8 K min^{-1}, 200°C to 250°C at 25 K min^{-1}, and 250°C for 6 min. The internal standard for the quantification of FFAs was heptadecanoic acid. The remaining 180 μL of the sample was used for the analysis of free oxylipin (Supplemental Table S1).

Statistical Analysis

Descriptive statistics including the mean and SE along with Tukey's range test for multiple comparison in conjunction with an ANOVA were used to determine significant differences. $P < 0.05$ was considered significant.

Supplemental Data

The following materials are available in the online version of this article.

Supplemental Figure S1. Overview of callose deposition in wheat spikes after fungal infection.

Supplemental Figure S2. Expression analysis of *TaGSL* genes in wheat spikes during fungal infection.

Supplemental Figure S3. Disease phenotypes of GFP-tagged and the respective untagged *F. graminearum* strains on wheat spikes.

Supplemental Figure S4. Rating of colonization severity after *F. graminearum* infection.

Supplemental Figure S5. Impact of α-linolenic acid (18:3) and 2-DDG on callose deposition in wheat spikes infected with *F. graminearum* Δ*fgl1*.

Supplemental Figure S6. Overview of FFAs and 2-DDG impact on the progress of *F. graminearum* infection in wheat spikes.

Supplemental Figure S7. α-Linolenic acid (18:3) and 2-DDG impact on infection severity and progress in wheat spikes inoculated with the GFP-tagged *F. graminearum* wild type.

Supplemental Figure S8. Growth assay on minimal medium supplemented with callose synthesis inhibitors.

Supplemental Figure S9. Callose deposition in wheat spikes after infection with the DON-deficient *F. graminearum* mutant.

Supplemental Figure S10. Expression analysis of *TaPR* genes in different sections of wheat spikes during *F. graminearum* infection.

Supplemental Figure S11. Purity and size of the lipase FGL1 from *F. graminearum*.

Supplemental Figure S12. Effect of lipase application on tissue degradation in wheat florets.

Supplemental Table S1. Concentration of FFAs and esterified fatty acids and oxylipins as well as salicylic acid in *F. graminearum*-infected wheat spike tissue.

Supplemental Table S2. Relative mycelium amounts in *F. graminearum*-infected wheat spike tissue.

Received January 25, 2014; accepted March 29, 2014; published March 31, 2014.

LITERATURE CITED

Aist JR, Williams PH (1971) The cytology and kinetics of cabbage root hair penetration by *Plasmodiophora brassicae*. Can J Bot **49:** 2023–2034

Aspinall GO, Kessler G (1957) The Structure of Callose from the Grape Vine. Chemistry and Industry, London

Bai GH, Desjardins AE, Plattner RD (2002) Deoxynivalenol-nonproducing *Fusarium graminearum* causes initial infection, but does not cause disease spread in wheat spikes. Mycopathologia **153:** 91–98

Bai GH, Shaner G (1994) Scab of wheat: prospects for control. Plant Dis **78:** 760–766

Barnes PJ (1982) Lipid composition of wheat germ and wheat germ oil. Fette Seifen Anstrichmittel **84:** 256–269

Baudouin E, Meskiene I, Hirt H (1999) Unsaturated fatty acids inhibit MP2C, a protein phosphatase 2C involved in the wound-induced MAP kinase pathway regulation. Plant J **20:** 343–348

Bayles CJ, Ghemawat MS, Aist JR (1990) Inhibition by 2-deoxy-D-glucose of callose formation, papilla deposition, and resistance to powdery mildew in an *ml-o* barley mutant. Physiol Mol Plant Pathol **36:** 63–72

Bravo-Ruiz G, Ruiz-Roldán C, Roncero MI (2013) Lipolytic system of the tomato pathogen *Fusarium oxysporum* f. sp. *lycopersici*. Mol Plant Microbe Interact **26:** 1054–1067

Brown I, Trethowan J, Kerry M, Mansfield J, Bolwell GP (1998) Localization of components of the oxidative cross-linking of glycoproteins and of callose synthesis in papillae formed during the interaction between non-pathogenic strains of *Xanthomonas campestris* and French bean mesophyll cells. Plant J **15:** 333–343

Brown NA, Antoniw J, Hammond-Kosack KE (2012) The predicted secretome of the plant pathogenic fungus *Fusarium graminearum*: a refined comparative analysis. PLoS ONE **7:** e33731

Buerstmayr H, Ban T, Anderson JA (2009) QTL mapping and marker-assisted selection for Fusarium head blight resistance in wheat: a review. Plant Breed **128:** 1–26

Cui X, Shin H, Song C, Laosinchai W, Amano Y, Brown RM Jr (2001) A putative plant homolog of the yeast beta-1,3-glucan synthase subunit FKS1 from cotton (Gossypium hirsutum L.) fibers. Planta **213:** 223–230

Davis KR, Litteneker N, LeTourneau D, McGinnis J (1980) Evaluation of the nutrient composition of wheat. I. Lipid constituents. Cereal Chem **57:** 178–184

Dean R, Van Kan JA, Pretorius ZA, Hammond-Kosack KE, Di Pietro A, Spanu PD, Rudd JJ, Dickman M, Kahmann R, Ellis J, et al (2012) The top 10 fungal pathogens in molecular plant pathology. Mol Plant Pathol **13:** 414–430

deBary A (1863) Recherches sur le développement de quelques champignons parasites. Ann Sci Nat Bot Biol Veg **20:** 5–148

del Blanco IA, Frohberg RC, Stack RW, Berzonsky WA, Kianian SF (2003) Detection of QTL linked to Fusarium head blight resistance in Sumai 3-derived North Dakota bread wheat lines. Theor Appl Genet **106:** 1027–1031

Desjardins AE, Proctor RH, Bairoch A, McCormick SP, Shaner G, Buechley G, Hohne TM (1996) Reduced virulence of trichothecene nonproducing mutants of *Giberella zeae* in wheat field tests. Mol Plant Microbe Interact **9:** 775–781

Dijkgraaf GJ, Abe M, Ohya Y, Bussey H (2002) Mutations in Fks1p affect the cell wall content of β-1,3- and β-1,6-glucan in *Saccharomyces cerevisiae*. Yeast **19:** 671–690

Doblin MS, De Melis L, Newbigin E, Bacic A, Read SM (2001) Pollen tubes of *Nicotiana alata* express two genes from different β-glucan synthase families. Plant Physiol **125:** 2040–2052

Douglas CM, Foor F, Marrinan JA, Morin N, Nielsen JB, Dahl AM, Mazur P, Baginsky W, Li W, el-Sherbeini M, et al (1994) The Saccharomyces cerevisiae FKS1 (ETG1) gene encodes an integral membrane protein which is a subunit of 1,3-beta-D-glucan synthase. Proc Natl Acad Sci USA **91:** 12907–12911

Ellinger D, Naumann M, Falter C, Zwikowics C, Jamrow T, Manisseri C, Somerville SC, Voigt CA (2013) Elevated early callose deposition results in complete penetration resistance to powdery mildew in Arabidopsis. Plant Physiol **161:** 1433–1444

Feng J, Wang F, Liu G, Greenshields D, Shen W, Kaminskyj S, Hughes GR, Peng Y, Selvaraj G, Zou J, et al (2009) Analysis of a *Blumeria graminis*-secreted lipase reveals the importance of host epicuticular wax components for fungal adhesion and development. Mol Plant Microbe Interact **22:** 1601–1610

Göbel C, Feussner I, Rosahl S (2003) Lipid peroxidation during the hypersensitive response in potato in the absence of 9-lipoxygenases. J Biol Chem **278:** 52834–52840

Guenther JC, Hallen-Adams HE, Bücking H, Shachar-Hill Y, Trail F (2009) Triacylglyceride metabolism by *Fusarium graminearum* during colonization and sexual development on wheat. Mol Plant Microbe Interact **22:** 1492–1503

Hong Z, Delauney AJ, Verma DP (2001) A cell plate-specific callose synthase and its interaction with phragmoplastin. Plant Cell **13:** 755–768

Jacobs AK, Lipka V, Burton RA, Panstruga R, Strizhov N, Schulze-Lefert P, Fincher GB (2003) An *Arabidopsis* callose synthase, GSL5, is required for wound and papillary callose formation. Plant Cell **15:** 2503–2513

Jansen C, von Wettstein D, Schäfer W, Kogel KH, Felk A, Maier FJ (2005) Infection patterns in barley and wheat spikes inoculated with wild-type and trichodiene synthase gene disrupted *Fusarium graminearum*. Proc Natl Acad Sci USA **102:** 16892–16897

Jones JD, Dangl JL (2006) The plant immune system. Nature **444:** 323–329

Kang Z, Buchenauer H (1999) Immunocytochemical localization of fusarium toxins in infected wheat spikes by *Fusarium culmorum*. Physiol Mol Plant Pathol **55:** 275–288

Kang Z, Buchenauer H (2000) Cytology and ultrastructure of the infection of wheat spikes by *Fusarium culmorum***.** Mycol Res **104:** 1083–1093

Kauss H, Jeblick W (1986) Influence of free fatty acids, lysophosphatidylcholine, platelet-activating factor, acylcarnitine, and echinocandin B on 1,3-β-D-glucan synthase and callose synthesis. Plant Physiol **80:** 7–13

Koh EJ, Zhou L, Williams DS, Park J, Ding N, Duan YP, Kang BH (2012) Callose deposition in the phloem plasmodesmata and inhibition of phloem transport in citrus leaves infected with "*Candidatus liberibacter asiaticus*." Protoplasma **249:** 687–697

Kouker G, Jaeger KE (1987) Specific and sensitive plate assay for bacterial lipases. Appl Environ Microbiol **53:** 211–213

Lamb C, Dixon RA (1997) The oxidative burst in plant disease resistance. Annu Rev Plant Physiol Plant Mol Biol **48:** 251–275

Li J, Burton RA, Harvey AJ, Hrmova M, Wardak AZ, Stone BA, Fincher GB (2003) Biochemical evidence linking a putative callose synthase gene with (1→3)-beta-D-glucan biosynthesis in barley. Plant Mol Biol **53:** 213–225

Madgwick JW, West JS, White RP, Semenov MA, Townsend JA, Turner JA, Fitt BDL (2011) Impacts of climate change on wheat anthesis and fusarium ear blight in the UK. Eur J Plant Pathol **130:** 117–131

Mangin L (1895) Recherches sur les Péronosporées. Bull Soc Hist Nat Autun **8:** 55–108

McMullen M, Jones RL, Gallenberg D (1997) Scab of wheat and barley: a reemerging disease of devastating impact. Plant Dis **81:** 1340–1348

Meyberg M (1988) Selective staining of fungal hyphae in parasitic and symbiotic plant-fungus associations. Histochemistry **88:** 197–199

Miedaner T, Reinbrecht C, Schilling AG (2000) Association among aggressiveness, fungal colonization, and mycotoxin production of 26 isolates of *Fusarium graminearum* in winter rye head blight. J Plant Dis Prot **107:** 124–134

Mims CW, Copes WE, Richardson EA (2000) Ultrastructure of the penetration and infection of pansy roots by Thielaviopsis basicola. Phytopathology **90:** 843–850

Murakami K, Chan SY, Routtenberg A (1986) Protein kinase C activation by cis-fatty acid in the absence of Ca^{2+} and phospholipids. J Biol Chem **261:** 15424–15429

Nishimura MT, Stein M, Hou BH, Vogel JP, Edwards H, Somerville SC (2003) Loss of a callose synthase results in salicylic acid-dependent disease resistance. Science **301:** 969–972

Østergaard L, Petersen M, Mattsson O, Mundy J (2002) An Arabidopsis callose synthase. Plant Mol Biol **49:** 559–566

Proctor RH, Hohn TM, McCormick SP (1995) Reduced virulence of Gibberella zeae caused by disruption of a trichothecene toxin biosynthetic gene. Mol Plant Microbe Interact **8:** 593–601

Ribichich KF, Lopez SE, Vegetti AC (2000) Histopathological spikelet changes produced by *Fusarium graminearum* in susceptible and resistant wheat cultivars. Plant Dis **84:** 794–802

Ruiz-Roldán MC, Maier FJ, Schäfer W (2001) PTK1, a mitogen-activated-protein kinase gene, is required for conidiation, appressorium formation, and pathogenicity of Pyrenophora teres on barley. Mol Plant Microbe Interact **14:** 116–125

Schroeder HW, Christensen JJ (1963) Factors affecting the resistance of wheat to scab caused by *Gibberella zeae*. Phytopathology **53:** 831–838

Schwessinger B, Ronald PC (2012) Plant innate immunity: perception of conserved microbial signatures. Annu Rev Plant Biol **63:** 451–482

Sellhorn GE, Youn B, Webb BN, Gloss LM, Kang C, Grimes HD (2011) Biochemical characterization, kinetic analysis and molecular modeling of recombinant vegetative lipoxygenases from soybean. Int J Biol **3:** 44–62

Sherwood RT, Vance CP (1976) Histochemistry of papillae formed in reed canarygrass leaves in response to noninfecting pathogenic fungi. Phytopathology **66:** 503–510

Stone BA, Clarke AE (1992) Chemistry and Biology of (1→3)-β-Glucans. La Trobe University Press, Bundoora, Australia

Tamir-Ariel D, Rosenberg T, Navon N, Burdman S (2012) A secreted lipolytic enzyme from *Xanthomonas campestris* pv. *vesicatoria* is expressed in planta and contributes to its virulence. Mol Plant Pathol **13:** 556–567

Verhagen J, Vliegenthart JF, Boldingh J (1978) Micelle and acid-soap formation of linoleic acid and 13-L-hydroperoxylinoleic acid being substrates of lipoxygenase-1. Chem Phys Lipids **22:** 255–259

Voigt CA, Schäfer W, Salomon S (2005) A secreted lipase of Fusarium graminearum is a virulence factor required for infection of cereals. Plant J **42:** 364–375

Voigt CA, Schäfer W, Salomon S (2006) A comprehensive view on organ-specific callose synthesis in wheat (*Triticum aestivum* L.): glucan synthase-like gene expression, callose synthase activity, callose quantification and deposition. Plant Physiol Biochem **44:** 242–247

Voigt CA, Somerville SC (2009) Callose in biotic stress (pathogenesis): biology, biochemistry and molecular biology of callose in plant defence: callose deposition and turnover in plant-pathogen interactions. *In* A Bacic, GB Fincher, BA Stone, eds, Chemistry, Biochemistry, and Biology of (1→3)-β-Glucans and Related Polysaccharides. Academic Press, Burlington, MA, pp 525–562

Weiland JJ, Steffenson BJ, Cartwright RD, Webster RK (1999) Identification of molecular genetic markers in Pyrenophora teres f. teres associated with low virulence on 'Harbin' barley. Phytopathology **89:** 176–181

Zadoks JC, Chang TT, Konzak DF (1974) A decimal code for the growth stages of cereals. Weed Res **14:** 415–421